Generation of spherical fast electron waves in the presence of preplasma in ultraintense laser-matter interaction

X. H. Yang[1], Y. Y. Ma[1], H. Xu[2], F. Q. Shao[1], M. Y. Yu[3], H. B. Zhuo[1], Y. Yin[1], A. P. L. Robinson[4], C. L. Tian[1], M. Borghesi[5]

[1]*College of Science, National University of Defense Technology, Changsha 410073, China*

[2]*College of Computer Science, National University of Defense Technology, Changsha 410073,China*

[3]*Department of Physics, Zhejiang University, Hangzhou 310027, China and Institut für Theoretische Physik I, Ruhr-Universität Bochum, D-44780 Bochum, Germany*

[4]*Central Laser Facility, STFC Rutherford Appleton Laboratory, Chilton, OX11 0QX, UK*

[5]*School of Mathematics and Physics, Queen's University of Belfast, Belfast BT7 1NN, UK*

I. Introduction

Fast electrons generation in ultraintense laser-solid interaction have been investigated extensively recently. The energy spectrum, spatial distribution and divergence angle of the energetic electrons can be significantly affected by the preplasma created by the inherent laser prepulse and/or spontaneous emissions from the lasing system. Thus, the effect of the preplasma should be considered in studies of fast electron generation from intense laser-solid target interaction.

Interaction of an intense laser pulse with a solid target having a large preplasma can involve nonlinear processes such as self-focusing, filamentation, hole-boring, etc. that can play important roles in the generation and propagation of fast electrons. It has been found that the fast electrons generated in the preplasma usually have a two-temperature Maxwellian distribution. The temperature of the high-energy component is much higher than the ponderomotive energy and it scales with the length L_p of the preplasma. The efficiency of laser-to-electron energy conversion should thus increase with L_p. Moreover, the spatial divergence of the fast electrons also increases with L_p. The quasistatic electric and magnetic fields spontaneously produced in the preplasma during the laser-plasma interaction can also affect the fast electron generation and transport. Most existing studies on fast electron generation are focused on the energy spectrum of the electrons and the efficiency of energy conversion from the laser to the latter. The spatial structure of the fast electrons is rarely investigated. Information on the spatial structure of the electrons can be useful in identifying their generation mechanisms and potential applications.

In this paper, we focus mainly on the spatial distribution of the fast electrons generated by an ultraintense laser pulse interacting with a solid target that has a subcritical preplasma. The electrons are heated efficiently and penetrate through the thin solid target, appearing in the target-rear vacuum region in a spherical distribution that is periodic at the laser wavelength. This phenomenon can be attributed to laser self-focusing in the preplasma and the $\vec{v}\times\vec{B}$ acceleration of the fast electrons in the intense self-generated magnetic field in the conical focusing region.

II. Simulation model and results

The generation of the spherical fast electron waves is studied by a relativistic 2D3V particle-in-cell (PIC) code. A plasma slab with density $50n_c$ and thickness $5\lambda_0$ is preceded by a subcritical preplasma. The density of the latter increases exponentially from $0.02n_c$ to n_c with a scale length $L_p = 8\mu m$. The plasma consists of electrons and aluminium ions with charge 10e. The initial temperature of both the electrons and ions is 1 KeV. A $10^{20} W/cm^2$ (a_0=8.54) *p*-polarized laser pulse is incident normally from the left. Both the spatial and temporal profiles of the laser pulse are Gaussian. The laser spot radius is $5\lambda_0$ and the pulse duration is $40T_0$.

In Fig. 1, one can see that a plasma channel is formed in the preplasma and several nonlinear processes take place there, including self-focusing, hole-boring, as well as filamentation, all of which can affect the generation and propagation of the fast electrons. The electrons are accelerated by the laser pulse as it propagates in the preplasma. The energetic electrons then penetrate the solid-density slab and enter into the backside vacuum region, where they exhibit a periodic spherical distribution with $0.2n_c$ density peaks and laser wavelength spacings. A laser pulse propagating in underdense plasma with a frequency of ω_p experiences relativistic self-focusing if the laser power *P* exceeds

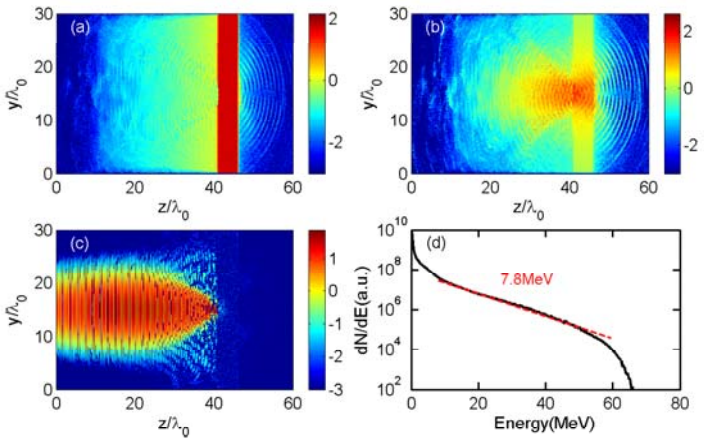

Fig. 1. $\log_{10}$ of electron density (a) and kinetic energy density (b) distribution at t=90T_0, respectively. log10 of Poynting vector along the laser propagation axis at t=70 T_0(c). The energy spectrum of electrons at t=100 T_0(d).

the critical power $P_{cr} \approx 17\left(\omega_0 / \omega_p\right)^2 GW$ [1]. For the average density ($\sim 0.25 n_c$) of the peplasma, we obtain $P_{cr} \approx 6.7 \times 10^{11} W$, so that the self-focusing condition is satisfied. It can be seen that, in Fig. 1(c) , the laser pulse is indeed self-focused in the preplasma, resulting in a tight focal spot ($\sim 2\mu m$) at the solid-slab front. As the laser pulse propagates through a focusing medium, the phase fronts will propagate slower at the center than at the edge, thus inducing a curvature in the phase front and causing the light to bend. We can indeed see that self-focusing bends the laser wave fronts to a converging spherical profile. Figure 1(b) shows that the fast electron layers in the upper (lower) vacuum regions behind the target are generated in the lower (upper) regions of the preplasma. That is, the fast electrons from the preplasma cross the midplane as they propagate through the solid target layer. This is because the laser-light polarization in the preplasma is locally modulated by the self-focusing, leading to a $\vec{v} \times \vec{B}$ force on the electrons that drives them towards the midplane and beyond, while the electrostatic space-charge field arising from the laser expulsion of the preplasma electrons confines the latter's transverse excursion. The electron temperature can reach 7.8 MeV, as can be seen in Fig.1(d), which is about two times of that given by the ponderomotive scaling.

Several mechanisms can produce high energy electrons in the underdense plasma. These include Betatron resonance absorption [2], stochastic heating, and laser wakefield acceleration (LWFA). In the present problem, the laser pulse duration is much larger than the plasma wavelength and the acceleration distance is very limited, so that the contribution of LWFA can be neglected. Stochastic heating can also be neglected. Figures 2(a) and 2(b) for the transverse and longitudinal electron phase space shows that the electrons oscillate in the laser electric field at the laser frequency. The transverse momentum of the electrons increases with the laser penetration distance and can reach a maximum of $\sim 70 m_e c$, which is about 8 times higher than that (namely $P_y = a_0 m_e c = 8.5 m_e c$) of a relativistic electron in a plane electromagnetic wave in vacuum [3]. Since the electrons are also accelerated

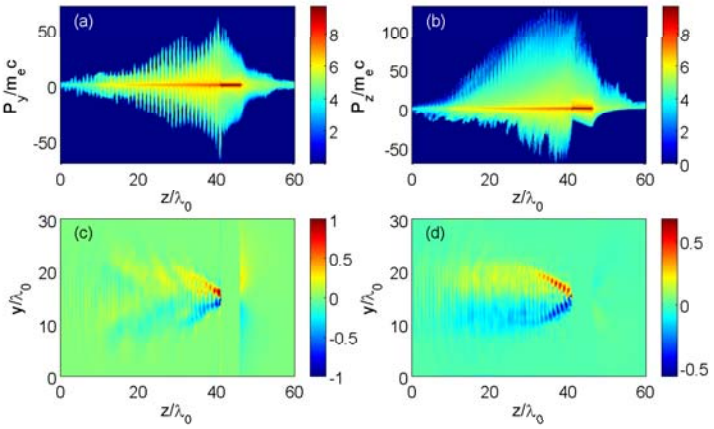

Fig. 2. Distribution of the electron transverse momentum (P_y) (a) and longitudinal momentum (P_z) (b), and the transverse quasistatic magnetic field (B_x) (c) and transverse electrostatic field (E_y) (d) at $t=80T_0$.

by the reflected laser pulse propagating backwards in the preplasma, as indicated by the negative electron momentum ($P_z < 0$) near the slab target in Fig. 2(b), their transverse momentum is further increased. The transverse electron momentum in the wave is converted into longitudinal momentum by the $\vec{v} \times \vec{B}$ force, and P_z of the fast electrons can reach $\sim 110 m_e c$, about 3 times that, namely $P_z = 1/2 a_0^2 m_e c = 36.5 m_e c$ in vacuum [3]. As expected, we see that the oscillation frequency of the longitudinal momentum is twice that of the transverse momentum, accompanied by significant longitudinal heating.

The ponderomotive expulsion of electrons and the action of the Lorentz force on them produce strong transverse charge-separation fields, as well as electron currents that generate quasistatic magnetic fields, as shown in Figs.2(c) and 2(d). We can see that the quasistatic fields E_y and B_x remain periodic in space (whose spatial periods are comparable to the laser wavelength), and their maximum amplitudes occur at the boundaries of the self-focusing cone, where the electron density is also the highest. Accordingly, electrons are accelerated forward in layers into the opposite half-space behind the target by the $v_y B_{xt}$ force (here B_{xt} should include both laser magnetic field and quasistatic field). This also explains why the spherical electron layers have a slight phase mismatch at the midplane.

III. Conclusion

Spherical electron waves generated are observed during an ultrainense laser interaction with a subcritical preplasma. The electrons are accelerated efficiently mainly due to the Betatron resonance absorption in the situations. The temperature of the fast electrons grows with increasing the preplasma scale length, which is much higher than that given by ponderomotive potential. The fast electrons can penetrate through the solid target and exhibit a spherical distribution with wavelength spacings behind the target, which could be mainly due to the self-focusing and the fast electrons experience both $\vec{v} \times \vec{B}$ and electrostatic force. The spherical wave reported here can be used for the production of spherical flying mirrors and have a potential of generation of ultra-short and bright radiation in the KeV range, such as hard x-ray.

References

[1] G. Sun et al., Phys. Fluids 30, 526 (1987)

[2] A. Pukhov et al., Phys. Plasmas 6, 2847(1999)

[3] W. Yu et al., Phys. Rev. Lett. 85, 570 (2000)